Raman spectroscopic monitoring of droplet polymerization in a microfluidic device†

Susan E. Barnes, Zuzanna T. Cygan, Jesse K. Yates, Kathryn L. Beers* and Eric J. Amis

Received 13th March 2006, Accepted 31st May 2006
First published as an Advance Article on the web 12th July 2006
DOI: 10.1039/b603693g

Microfluidic methodologies are becoming increasingly important for rapid formulation and screening of materials, and development of analytical tools for multiple sample screening is a critical step in achieving a combinatorial 'lab on a chip' approach. This work demonstrates the application of Raman spectroscopy for analysis of monomer composition and degree of conversion of methacrylate-based droplets in a microfluidic device. Droplet formation was conducted by flow focusing on the devices, and a gradient of component composition was created by varying the flow rates of the droplet-phase fluids into the microchannels. Raman data were collected using a fiber optic probe from a stationary array of the droplets/particles on the device, followed by partial least squares (PLS) calibration of the first derivative (1600 cm^{-1} to 1550 cm^{-1}) allowing successful measurement of monomer composition with a standard error of calibration (SEC) of $\pm 1.95\%$ by volume. Following photopolymerization, the percentage of double bond conversion of the individual particles was calculated from the depletion of the normalized intensity of the C=C stretching vibration at 1605 cm^{-1}. Raman data allowed accurate measurement of the decrease in double bond conversion as a function of increasing crosslinker concentration. The results from the research demonstrate that Raman spectroscopy is an effective, on-chip analytical tool for screening polymeric materials on the micrometre scale.

Introduction

Over the last decade there have been significant advances in the use of microfluidic devices to perform chemical analysis and reactions on the micrometre scale.[1] To date, microfluidic technology has found numerous applications in the pharmaceutical,[2] life sciences and microelectronics industries.[3] It is utilized as a technique for performing biological assays and high-throughput screening for combinatorial syntheses.[4–7]

Technology development in this field has been driven by the rewards gained from the use of microanalysis in replacement of its conventional macro-scale analogues. The main advantages of these methodologies include: increased ease of fluid manipulation, low reagent consumption and increased analysis efficiency.[2]

The small sample volumes associated with microfluidics demand the implementation of sensitive analytical techniques for on-chip characterization of chemical species. The development and application of micro-instrumentation for monitoring of material properties and reactions on the microlitre scale is a rapidly developing area. On-going research, including work presented by the New Sampling/Sensor Initiative (NeSSI), involves adaptation of emerging ''lab on a chip'' sensors into miniaturized modular manifolds to produce integrated micro-analytical devices.[8–11]

In the field of materials science, a number of spectroscopic methods have been applied for on-chip analysis including fluorescence microscopy,[12] UV-visible absorption spectroscopy,[13] confocal Raman microscopy[12,14–17] and surface enhanced resonant Raman scattering (SERRS).[18,19] However, these techniques have been largely used for analysis of aqueous systems and laminar flows. Also, in many cases, the size and expensive nature of the monitoring equipment is extreme, considering its analytical applications. This current study demonstrates the application of low resolution, fiber optic Raman spectroscopy as a relatively inexpensive, portable technique for screening of polymeric systems inside of microfluidic channels.

Raman spectroscopy offers a number of advantages over other spectroscopic methods available for in-situ analysis of polymers, including its high sensitivity to a range of organic molecules and low sensitivity to water. The use of fiber optic Raman in a back-scattering geometry allows versatile, non-invasive detection of materials without interrupting the flow or progress of a chemical reaction. There is a wealth of literature available on the application of Raman spectroscopy for analysis of polymer composition and conversion in bulk reactions.[20–24] The work presented in this manuscript details the application of Raman spectroscopy for analysis of these parameters in micron-sized (250 μm to 400 μm) monomer/polymer droplets produced inside a microfluidic device. During formulation and analysis, droplets are suspended in an aqueous surfactant continuous phase. The low sensitivity of Raman scatter to water, as opposed to other similar analysis

NIST Combinatorial Methods Center, Polymers Division, National Institute of Standards and Technology, 100 Bureau Drive, Gaithersburg, MD, 20879-8542, USA. E-mail: beers@nist.gov; Fax: +1 301 975 4924; Tel: +1 301 975 2113

techniques such as infrared spectroscopy, makes this an excellent analytical tool for characterization of this system. The microfluidic devices utilized were low cost disposable thiolene-based devices that have high stability to a number of organic solvents making them suitable for use with polymer systems.[25] Thiolene devices allow rapid prototyping of a range of devices with different designs. The flexibility and simplicity of the fabrication process allows production of devices that best fit the experimental protocol and the analytical tools applied.[26]

The formation of droplets in microchannels which contain multiple reagents of varying compositions has been presented by a number of research groups.[27–29] Several groups have also demonstrated the use of microfluidic devices as platforms for photopolymerization of monomer droplets to produce polymer particles.[30–35] The formulation of droplets facilitates mixing and encapsulation of individual 'packets' of monomer compositions, which allows ease of sample manipulation, especially in the case of highly viscous or solid cross-linked particles.[36]

In this study, arrays of organic phase droplets have been generated containing a range of methacrylate based monomer/dimethacrylate crosslinker compositions. Raman spectroscopy has been applied as an on-chip tool for validation and measurement of the monomer composition across the array. Raman spectra were subsequently acquired from the polymer particles following photopolymerization. The data were used for quantitative analysis of conversion as a function of the droplet composition. Gaining an understanding of the relationship between these two properties is imperative to the design of dental materials, where leaching of residual monomer is undesirable.

The model methacrylate systems analyzed are comparable to those studied for components of dental composites, where analysis of composition and conversion is critical for successful formulation development.[37] Dental restorative composites are complex systems whose properties are influenced by a range of chemical and processing parameters.[38] Such dental resins are often comprised of a binary or ternary mixture, where the material properties and processability can be easily altered by changes in the formulation.[39] A number of sucessful studies have been reported using Raman spectrosopy for analysis of the degree of conversion of commerical dental composites.[40,41] Micro-Raman spectroscopy has also been applied in order to study adhesvie distribution within the resins,[42,43] and for determination of the extent of monomer conversion from the surface to the bulk of cured resin samples.[44]

Experimental‡

Devices and materials

Microfluidic devices were fabricated from a thiolene-based optical adhesive and two 1 mm thick borosilicate slides (Borofloat, Cincinnati Gasket). Borosilicate glass slides (75 mm × 50 mm) were chosen in place of standard glass microscope slides to minimize fluorescence effects in the Raman data. Further details of the device fabrication can be reviewed in recent publications.[25,26] Fig. 1 is a schematic layout of the channel design. All channel depths were 500 μm, with channel widths of 700 μm (Fig. 1A), except for the constriction at the flow focusing junction which was 250 μm (Fig. 1B), and the switch back portion of the device (Fig. 1C) where the channels were increased to 1400 μm for collection of the droplet array. The device possessed two inputs for organic solutions (one per constituent) and two aqueous phase inputs. Solutions were introduced into the device using programmable syringe pumps (Braintree Scientific BS 8000).

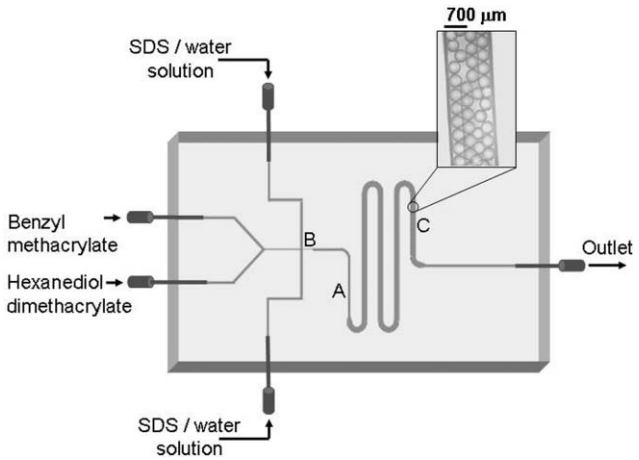

Fig. 1 Schematic of a thiolene-based microfluidic device used for droplet formulation. All channels were set to a depth of 500 μm but varied in width from 250 μm (B) to 1400 μm (C).

Benzyl methacrylate monomer (BZMA, Rohm Tech Monomers) and 1,6-hexanediol dimethacrylate crosslinker (HDMA, Esstech) were used as components for organic droplet formation. Solutions were purged with nitrogen before use to decrease oxygen inhibition of the photopolymerization. All monomer compositions are expressed as % by volume of the organic phase only, not regarding the aqueous fraction of the two phase mixture. Droplets were created at a flow focusing junction in the device,[45] and suspended in a matrix of water containing 9 mM sodium dodecyl sulfate (SDS, Fluka). A gradient in droplet composition was achieved by stepping the syringe pump flow rates of the organic phases with respect to one another while maintaining a constant total organic phase flow rate (0.032 mL min^{-1}). A constant aqueous phase flow rate (0.1 mL min^{-1}) was maintained throughout. Both organic phases contained 1% by mole of Irgacure 819 photoinitiator (Ciba Specialty Chemicals). Particles produced at each composition were polydisperse, varying in diameter from 400 μm to 250 μm before polymerization (the lower limit of the droplet size was fixed to accommodate the focal size of the Raman probe), as observed by optical microscopy.[25]

Following gradient formation, flow was halted, and the droplets collected on the device for analysis. All the outlets on the device were subsequently sealed to prevent evaporation. Fig. 2 shows a typical experimental set-up for data acquisition and polymerization of the droplets on the microfluidic device.

‡ Certain equipment, instruments or materials are identified in this paper in order to adequately specify the experimental details. Such identification does not imply recommendation by the National Institute of Standards and Technology nor does it imply the materials are necessarily the best available for the purpose.

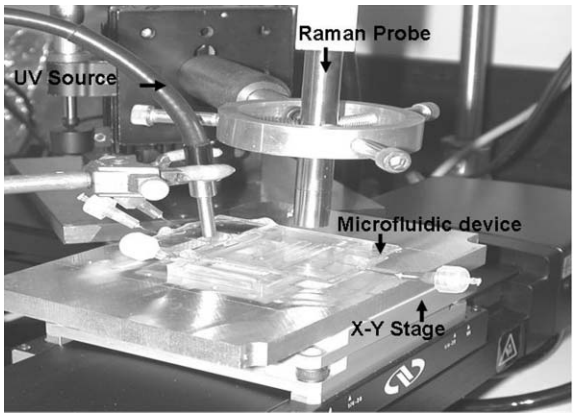

Fig. 2 Experimental set-up for Raman analysis and photopolymerization of methacrylate monomer droplets in a thiolene-based microfluidic device.

Raman spectroscopy

Raman spectra were obtained using a R2001 spectrometer (Raman systems) with 785 nm laser excitation and CCD detection. Spectra were collected up to 2500 wavenumbers (cm^{-1}) using a non-contact fiber optic probe with a nominal focal length of 5 mm and 200 μm focal spot size. Spectra were acquired by focusing the fiber optic probe, positioned above the device, into the microchannel through the top surface. Movement of the device beneath the probe using a translational *x*-*y* stage allowed location of individual monomer droplets. The fine focusing of the Raman probe in the *z*-direction was controlled and measured by a barrel micrometer.

All spectra were acquired over three minutes (180 s exposure time over 1 accumulation) at a nominal resolution of 10 cm^{-1}. Scanning times were chosen to acquire an acceptable signal-to-noise for accurate data analysis. Scanning of individual droplets in the gradient was conducted before and 24 hours after photopolymerization to determine the extent of final double bond conversion.

A series of reference spectra were acquired from droplets of known monomer concentration for calibration purposes. These droplets were formulated, and standard data acquired during a series of individual experiments on the same device. Data were collected from droplets with monomer compositions of 100, 75, 60, 50, 25, and 10% by volume BZMA (8 samples per data set). Univariate and multivariate calibrations of the data were constructed and subsequently used to determine the monomer composition of the droplets along the microchannel gradient. All data were pre-treated by background subtraction of the spectrum of the micro-channel containing only SDS–water solution, acquired through the top borosilicate surface of the device.

Spectra are plotted in Raman shift (cm^{-1}) from the incident radiation (785 nm). Commercial software (Grams 32/AI, Galactic Industries Corp.) was used to process spectral data, and all chemometric analysis was conducted using partial least squares (PLS) regression. [46–48]

Photopolymerization

Photopolymerization of the droplets was initiated at 5000 mW cm^{-2} using a UV lamp (EXFO Novacure 2100) coupled to a fiber optic probe (spot size ~2 mm). The probe was positioned flush with the top surface of the device, and the device was translated beneath the probe twice using an *x*-*y* stage at a rate of 1 mm s^{-1}. This methodology ensured uniform exposure of all droplets throughout the channels. Dispersion of the excitation radiation through the device during irradiation at individual locations effectively extended the overall dosing time for each droplet. Additional doses, applied after monitoring the conversion, ensured that maximum conversion was achieved.

Results and discussion

The molecular structures of the two components used for formulation of the droplet gradient are shown in Fig. 3 along with their associated Raman spectra (2000 cm^{-1} to 150 cm^{-1}). Clear differences in the spectra of each component can be observed in the data, particularly in the double bond region (1800 cm^{-1} to 1550 cm^{-1}).

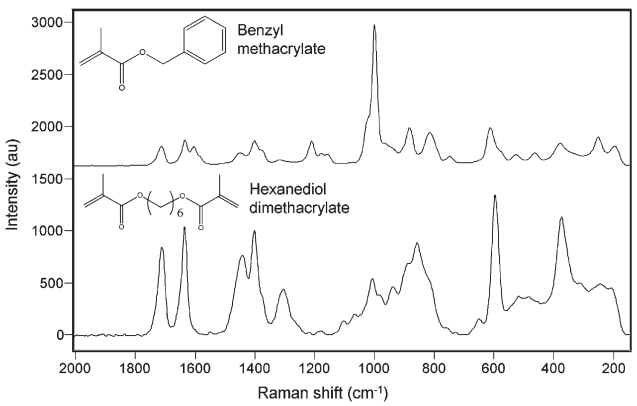

Fig. 3 Off-set Raman spectra (3 minute, 1 accumulation) and associated molecular structures of the monomer and crosslinker components used in droplet formation.

Fig. 4 shows an on-chip Raman spectrum acquired from a droplet containing 100% by volume BZMA. The data is shown before and after manipulation.

A fluctuating baseline was observed in the raw data, predominately caused by scatter of the incident radiation from the upper slide of the device (Fig. 4A). Background subtraction of the spectrum of the microchannel containing SDS solution (acquired through the top surface), coupled with a 5 point linear baseline correction, allowed more accurate data analysis and interpretation (Fig. 4B).

A series of reference spectra were acquired from droplets containing known monomer concentrations for calibration purposes. Fig. 5 is a stack plot of a series of Raman spectra (1900 cm^{-1} to 550 cm^{-1}) acquired from individual droplets of known monomer concentrations (10, 25, 50 and 75% by volume BZMA). Significant increases in the absolute intensity of spectral features corresponding to the phenyl group vibrations of the BZMA can be seen as the monomer content increases.

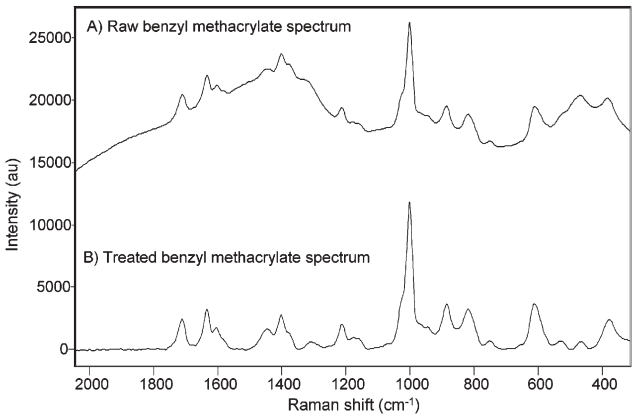

Fig. 4 Off-set on-chip Raman spectra of a benzyl methacrylate droplet; (A) before and (B) after data manipulation by background subtraction and linear baseline correction.

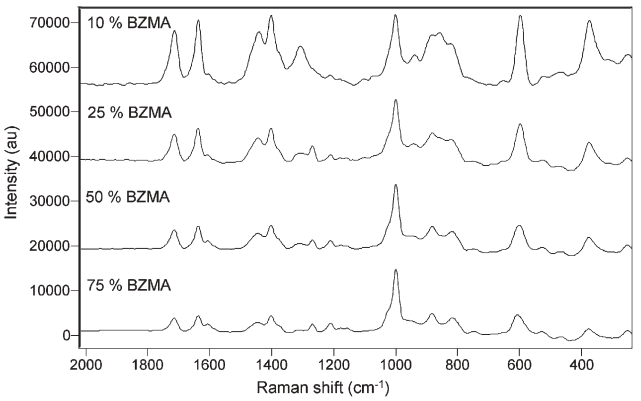

Fig. 5 Stack plot of on-chip Raman spectra acquired from droplets of known monomer concentrations. Data acquired for 3 minutes over one accumulation.

Most notably, an increase in the intensity of the C=C ring stretching modes at 1605 cm^{-1} and 1582 cm^{-1}, and in the ring breathing mode at 1000 cm^{-1} are observed.[49,50] The second quadrant stretching band at 1582 cm^{-1} is of much lower relative intensity than the first, and at low BZMA compositions is difficult to resolve from the baseline. An increase in intensity of the feature at 1210 cm^{-1}, ascribed to the C_6H_5–C vibration of the benzyl methacrylate, can also be observed as the monomer content of the droplets is increased.[51] A gradual shift in the wavenumber of the C–C=O stretching mode from 612 cm^{-1} to 595 cm^{-1} was seen as the composition of the droplets changed from 100% by volume benzyl methacrylate monomer to 100% by volume 1,6-hexanediol dimethacrylate cross-linker.

In the absence of an internal reference band in the Raman data, the ratio of the C=C ring stretching mode intensity (1605 cm^{-1}) to that of the vinylic C=C stretching mode at 1636 cm^{-1} (present in the spectra of both the monomer and crosslinker) was used to create a calibration for monomer content prediction. For this system, the intensity ratio of these two bands showed a linear relationship with change in monomer content (% by volume) over the entire concentration range analyzed (R^2 = 0.998). All data were background subtracted and baseline corrected before measurement of the relevant band intensities. The standard error of calibration (SEC) for the least squares calibration constructed was calculated as $\pm$1.42% by volume BZMA (standard uncertainty of 1σ) from cross validation of the spectra with the model itself. The application of band ratio techniques for determination of component composition, in the absence of an internal reference, has been demonstrated in previous publications.[23]

The overlapping nature of the bands in the double bond stretching region (1800 cm^{-1} to 1550 cm^{-1}) of the data made absolute intensity measurements or peak integration analysis complex and time consuming. Partial least squares (PLS) analysis was adopted in an attempt to better model the variations in the data. Chemometric analysis allows robust modeling of the full number of variations in the spectral data set,[46–48] and was hence expected to provide a more robust calibration of monomer composition. A regression model was constructed using a training data set comprised of the reference spectra with their associated known monomer composition values. Data were mean-centered before analysis to enhance any spectral differences. The optimum PLS model (using PLS 1) for determination of BZMA content was created from calculating the first derivative of the data (Savitsky Golay method, 11 points, 2nd order polynomial) in the wavenumber region 1800 cm^{-1} to 1500 cm^{-1}. Calculation of the second derivative of the data did not significantly reduce the error associated with the model.

Calculation of the first derivative was observed to significantly reduce the effects of the baseline shifts and background variation in the spectra.[52] Fluctuations in background were ascribed to scatter of the incident radiation from the top surface of the device. This was seen to vary with differences in the level of the fiber optic with respect to the device surface.

The optimum number of factors required to model the full variation in the droplet spectra was determined to be four, from the predicted residual sum of squares (PRESS) plot of the data. However most of the variance in the spectral data set (96%) was modeled by the first two factors/eigenvectors. The SEC for the model was calculated to be $\pm$1.95% by volume BZMA (standard uncertainty of 1σ) by cross validation of the training spectra with the model itself. This error is marginally higher than that observed for the univariate calibration constructed from the peak ratio values. Fig. 6 shows the plot of the actual BZMA concentrations *versus* those predicted by the model. Generally, good agreement can be observed between the two sets of values, although some spread is observed in the individual data sets (single BZMA content droplets).

Differences in the absolute intensity of the Raman spectra within each data set were seen due to changes in sample volume from droplet to droplet (due to droplet size polydispersity). In the absence of an internal reference peak, these changes in intensity could not be normalized from the data. Using a calibration with four factors successfully modeled most of the variation in the data including those occurring due to sample volume changes, however it appears that adopting a band ratio technique was more effective in reducing scatter in the data from these affects.

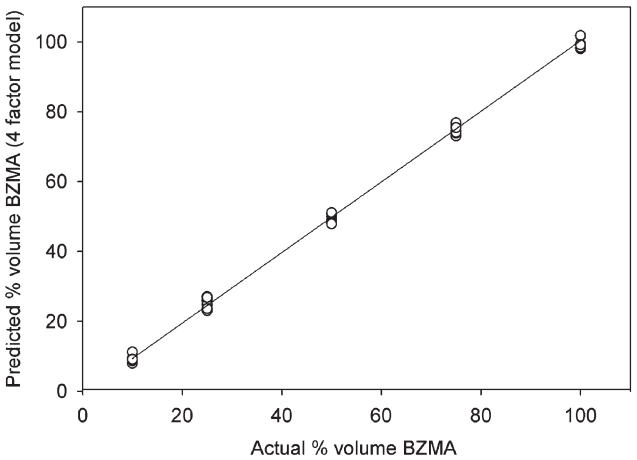

Fig. 6 Plot of actual and predicted % volume benzyl methacrylate for a 4-factor PLS model of the Raman spectra of monomer/crosslinker droplets.

Slight wavelength shifts were also observed in the experimental data as a consequence of the low instrument resolution. These shifts in wavelength had a greater impact on the error of chemometric calibration than for that associated with the absolute peak intensity measurements made for the linear regression analysis.

Following construction of the composition calibration, spectra of the droplets formed in the gradient were acquired; the data were analyzed and subsequently related to the calibrations. Fig. 7 is a plot of the composition of BZMA in individual droplets as a function of their position (mm) in the array as determined by calibrations constructed from both least squares regression of the peak ratios and from PLS analysis of the data.

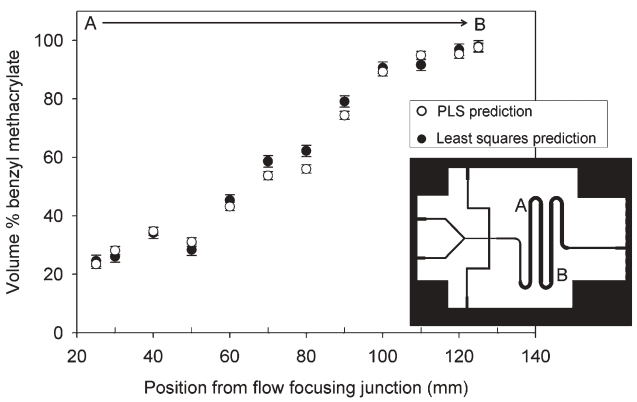

Fig. 7 Plot of benzyl methacrylate composition in individual droplets as a function of their position in the microchannel gradient (mm). Inset is a schematic drawing of the device design; (A) position of first droplet analyzed, (B) position of last droplet in the array.

Both forms of data analysis identify the presence of a gradient of monomer concentration in the microchannels as anticipated. Good agreement is seen between monomer compositions determined for the droplets in the gradient which extends from approximately 23% by volume to 98% by volume BZMA. Slight differences are observed between the calculated compositions of droplets in the center of the gradient (70 mm to 90 mm into the array).

Following confirmation and measurement of the composition gradient in the channels, photopolymerization of the droplets was initiated. Raman data were acquired 24 h after photoinitiation at the same channel locations as the initial pre-cure data, to calculate the extent of full double bond conversion. Data were also re-acquired after 48 h to confirm that 24 h was an adequate time frame for the polymerization to be complete.

Fig. 8 shows the change in the Raman spectra (1800 cm^{-1} to 700 cm^{-1}) as a function of cure for two droplets containing 91.65% by volume and 24.60% by volume benzyl methacrylate, respectively.

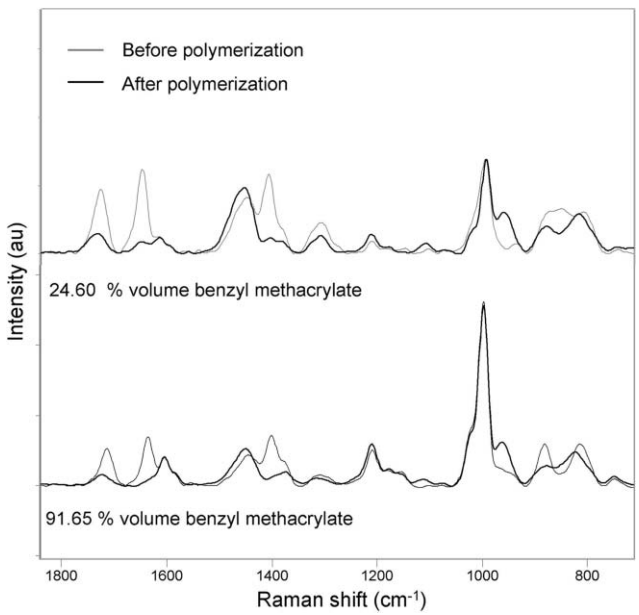

Fig. 8 Off-set normalized Raman spectra from before and 24 h after photopolymerization, with data shown for droplets containing 91.65% by volume and 24.60% by volume benzyl methacrylate.

Normalized data are shown for each droplet before and 24 h after photopolymerization. Data were normalized to the intensity of the phenyl ring stretching vibration (1605 cm^{-1}).[53] Pronounced differences can be observed specifically in the carbonyl and double bond stretching region of the spectra (1800 cm^{-1} to 1550 cm^{-1}). Both sets of spectra illustrate that the intensities of the phenyl ring stretching modes (1605 cm^{-1} and 1582 cm^{-1}) and the ring breathing mode (1000 cm^{-1}) remain the same before and after photopolymerization, making these features suitable for normalization purposes. There is a notable decrease in the intensity of the vinyl C=C double bond stretch (1635 cm^{-1}) upon curing of droplets of both compositions. This decrease in band intensity is more pronounced in the spectra of the droplets with higher BZMA monomer content.

The decrease in the relative intensity of the double bond stretch was used to calculate the extent of conversion for each discrete droplet of pre-determined composition. Individual sets of before and after data (for each individual droplet analyzed) were normalized to the intensity of the phenyl ring stretching

vibration (1605 cm^{-1}).[42] Normalization to this band was found to provide an accurate and repeatable measurement of conversion ($\pm 2\%$; standard uncertainty of 2σ). Normalization of the spectral data to the carbonyl stretching band was not possible, as a wavenumber shift (1712 cm^{-1} to 1724 cm^{-1}) and depletion in band intensity was observed on polymerization, ascribed to the loss of conjugation of the carbonyl group with the double bond.[21]

Fig. 9 shows the calculated double bond conversion (%) as a function of BZMA composition as determined from the Raman data. The extent of conversion increases from 78% at low BZMA concentrations to 95% at higher concentrations.

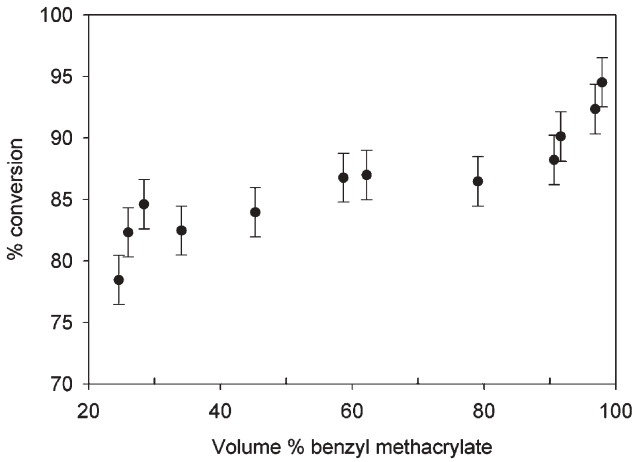

Fig. 9 Plot of the change in the % conversion of droplets in the microchannel gradient as a function of % by volume benzyl methacrylate.

These data show that for this monomer/crosslinker system, increasing the 1,6-hexanediol dimethacrylate cross-linker concentration reduces the overall degree of conversion. The result is as one would expect; an increase in the concentration of the crosslinker limits diffusion of the reactive species during polymerization. In addition, when one of the double bonds of the dimethacrylate has reacted following photoinitiation, a second pendant double bond remains which has very low mobility and is consequently easily trapped and restricted from reacting further.[54] The kinetics of such polymerization reactions rely on a number of influencing factors arising from the nature and functionality of the co-monomers and the extent of cross-linking.[55,56] Due to the complex chemistry and the difficulty in modeling free radical polymerizations, experimental measurements are key for gaining enhanced understanding. Therefore, a rapid screening method, such as Raman, is a valuable tool for efficient acquisition of empirical data.

The microfluidic technique that we have developed enables tailoring of the size and scope of the array of particles prepared within the device. Here, fifteen different compositions in a series of samples covering a broad range of many monomer-to-crosslinker ratios have been polymerized under identical conditions to provide experimental understanding of the system response to UV curing. For a two monomer mixture, this provides ample coverage of the parameter space of interest without over-sampling and excessive data. For systems with narrower regions of interest, or a more complex parameter space, the device and flow conditions can be re-engineered to accommodate larger sample sets.

Conclusions

The present study has shown the application of low resolution, fiber optic Raman spectroscopy as a technique for on-chip, quantitative analysis of monomer/polymer droplets in a microfluidic device. Good quality data have been acquired using a relatively low cost, versatile, low resolution instrument whose size is suited to the application and the environment in which it is utilized. Data acquired from small sample volumes show high signal-to-noise and good repeatability. Despite limited precision, the Raman data acquired has allowed successful mapping of droplet composition and conversion with acceptable accuracy and in a suitable time frame for combinatorial materials screening. Further development of the Raman instrumentation will increase the precision and versatility of the technique.

Both univariate and multivariate calibrations have allowed measurements of droplet composition to an accuracy of $\pm 1.42\%$ by volume and $\pm 1.95\%$ by volume BZMA, respectively. Good agreement between the composition gradient determined by the two data analysis techniques was observed despite the lack of an internal reference in the working system. The technique has further been shown to be an effective screening method for measurement of the extent of double bond conversion following UV cure.

The geometry of the fiber optic probe used for the measurements has allowed Raman spectroscopy to be utilized as a non-invasive measurement of polymer formulation properties. The relative insensitivity of Raman measurements to water has allowed application of this analytical technique for analysis of polymer droplets suspended in aqueous solution.

A limiting factor with this application is the comparatively long acquisition times required for data acquisition (3 min). This limits the experimental procedure to the analysis of droplets held in stationary arrays on the device, measurement of only late stage conversion, or monitoring of relatively slow polymerization reactions. The data acquisition time may be reduced by substituting the borosilicate substrate currently used with quartz slides to reduce the background in the Raman data. Also, the experimental approach can be adjusted to acquire high-throughput data from flowing droplets. Here a number of droplets of individual composition can be analyzed by averaging data acquired over many accumulations at short exposure times. Droplets may then be colleted away from the device for further analysis. These results describe a platform for the extension of Raman and other spectroscopic techniques such as near- and mid-infrared for near real-time, on-chip screening of polymeric reactions and other material properties.

Acknowledgements

The authors thank Dr Joseph Antonucci and Dr Sheng Lin-Gibson for helpful discussions and information as well as the generous donation of monomers used in these experiments. Thank you also to Dr Thomas Epps III for his scientific input.

Zuzanna Cygan was supported by a National Research Council Postdoctoral Fellowship.

This work was carried out at the NIST Combinatorial Methods Center (NCMC; www.nist.gov/combi).

References

1 T. Vilkner, D. Janasek and A. Manz, *Anal. Chem.*, 2004, **76**, 3373.
2 J. W. Hong and S. Quake, *Nat. Biotechnol.*, 2003, **21**, 1179.
3 J. Atencia and D. J. Beebe, *Nature*, 2005, **437**, 7059, 648.
4 E. J. Amis, *Nat. Mater.*, 2004, **3**, 2, 83.
5 H. A. Stone and S. Kim, *AIChE J.*, 2001, **47**, 1250.
6 P. Mitchell, *Nat. Biotechnol.*, 2001, **19**, 717.
7 C-C. Lee, G. Sui, A. Elizarov, C. J. Shu, Y.-S. Shin, A. N. Dooley, J. Huang, A. Daridon, P. Wyatt, D. S. Hartmuth, C. Kolb, O. N. Witte, N. Satyamurthy, J. R. Heath, M. E. Phelps, S. R. Quake and H.-R. Tseng, *Science*, 2005, **310**, 1793.
8 M. V. Koch and B. J. Marquardt, *J. Proc. Anal. Technol.*, 2004, **1**, 2, 12.
9 R. Yotter, L. Lee and D. Wilson, *IEEE Sens. J.*, 2004, **4**, 4, 395.
10 R. D'Aquino, *Chem. Eng. Prog.*, 2003, **99**, 12, 9.
11 P. Hollywood, *ARC Strategies*, 2004.
12 T. Park, M. Lee, J. Choo, Y. S. Kim, E. K. Lee, D. J. Kim and S. H. Lee, *Appl. Spectrosc.*, 2004, **58**, 10, 1172.
13 H. Lu, M. A. Schmidt and K. F. Jensen, *Lab Chip*, 2001, **1**, 22.
14 J. B. Salmon, A. Ajdari, P. Tabeling, L. Servant, D. Talaga and M. Joanicot, *Appl. Phys. Lett.*, 2005, **86**, 094106.
15 J. P. Lee, H. Rhee, J. Choo, Y. G. Chai and E. K. Lee, *J. Raman Spectrosc.*, 2003, **34**, 737.
16 P. D. I. Fletcher, S. J. Haswell and X. Zhang, *Electrophoresis*, 2003, **24**, 3239.
17 S.-A. Leung, R. F. Winkle, R. C. R. Wootton and A. J. deMello, *Analyst*, 2005, **130**, 46.
18 F. T. Docherty, P. B. Monaghan, R. Keir, D. Graham, W. E. Smith and J. M. Cooper, *Chem. Commun.*, 2004, **1**, 118.
19 R. M. Connatser, L. A. Riddle and M. J. Sepaniak, *J. Sep. Sci.*, 2004, **27**, 17–18, 1545.
20 T. R. McCaffery and Y. G. Durant, *J. Appl. Polym. Sci.*, 2002, **86**, 1507.
21 A. Al-Khanbashi, M. Dhamdhere and M. Hansen, *Appl. Spectrosc. Rev.*, 1998, **33**, 115.
22 M. van den Brink, M. Pepers, A. M. van Herk and A. L. German, *Macromol. Symp.*, 2000, **150**, 121.
23 N. Everall and B. King, *Macromol. Symp.*, 1999, **141**, 103.
24 N. Everall, Raman spectroscopy of synthetic polymers, in *Analytical Applications of Raman Spectroscopy*, ed. M. J. Pelletier, Blackwell Science Ltd, London: 1999, 127.
25 Z. T. Cygan, J. T. Cabral, K. L. Beers and E. J. Amis, *Langmuir*, 2005, **21**, 3629.
26 C. Harrison, J. T. Cabral, C. M. Stafford, A. Karim and E. J. Amis, *J. Micromech. Microeng.*, 2004, **14**, 153.
27 H. Song, M. R. Bringer, J. D. Tice, C. J. Gerdts and R. F. Ismagilov, *Appl. Phys. Lett.*, 2003, **83**, 4664.
28 J. D. Tice, H. Song, A. D. Lyon and R. F. Ismagilov, *Langmuir*, 2003, **19**, 9127.
29 M. Joanicot and A. Ajdari, *Science*, 2005, **309**, 887.
30 S. Sugiura, M. Nakajima and M. Seki, *Ind. Eng. Chem. Res.*, 2002, **41**, 4043.
31 Z. Nie, S. Xu, M. Seo, P. C. Lewis and E. Kumacheva, *J. Am. Chem. Soc.*, 2005, **127**, 8058.
32 S. Xu, Z. Nie, M. Seo, P. C. Lewis, E. Kumacheva, H. A. Stone, P. Garstecki, D. B. Weibel, I. Gitlin and G. M. Whitesides, *Angew. Chem., Int. Ed.*, 2004, **43**, 2.
33 D. Dendukuri, K. Tsoi, T. A. Hatton and P. S. Doyle, *Langmuir*, 2005, **21**, 2113.
34 P. C. Lewis, R. R. Graham, Z. Nie, S. Xu, M. Seo and E. Kumacheva, *Macromolecules*, 2005, **38**, 4536.
35 Z. Nie, S. Xu, M. Seo, P. C. Lewis and E. Kumacheva, *J. Am. Chem. Soc.*, 2005, **127**, 8058.
36 J. Takagi, M. Yamada, M. Yasuda and M. Seki, *Lab Chip*, 2005, **5**, 778.
37 J. M. Antonucci and J. W. Stansbury, in *Molecularly Designed Dental Polymers*, ed. R. Arshady, Washington DC, 1997.
38 V. Narayanan and AB. Scranton, *Trends Polym. Sci.*, 1997, **5**, 12, 415.
39 S. Lin-Gibson, F. A. Landis and P. L. Drzal, *Biomaterials*, 2006, **27**, 1711.
40 W. S. Shin, X. F LI, B Schwartz, S. L. Wunder and G. R. Baran, *Dent. Mater.*, 1993, **9**, 5, 317.
41 N. Emami and K.-J. M. Söderholm, *Eur. J. Oral Sci.*, 2003, **111**, 536.
42 C. Pianelli, J. Devaux, S. Bebelman and G. Leloup, *J. Biomed Mater. Res., Part B*, 1999, **48**, 5, 675.
43 B. Van Meerbeek, H. Mohrbacher, J. P. Celis, J. R. Roos, M. Braem, P. Lambrechts and G. Vanherle, *J. Dent. Res.*, **72**, 1423–1428.
44 M. A. Gauthier, I. Stangel, T. H. Ellis and X. X. Zhu, *J. Dent. Res.*, 2005, **84**, 8, 725.
45 S. L. Anna, N. Bontoux and H. A. Stone, *Appl. Phys. Lett.*, 2003, **82**, 364–366.
46 R. Winzen and H. M. Heise, Fundamental Chemometric Methods, in *Near-Infrared Spectroscopy; Principles, Instruments, Applications*, ed. Y. Ozaki, H. W. Siesler, S. Kawata, H. M. Heise, Wiley-VCH, New York, 2002.
47 J. Shaver, Chemometrics for Raman Spectroscopy, in *Handbook of Raman spectroscopy: From the research laboratory to the process line*, ed. I. R. Lewis, H. G. M. Edwards, Marcel Dekker, New York, 2001.
48 A. D. Walmsley, ''Chemometrics and Data treatment.'' in *Spectroscopy In Process Analysis*. ed. J. M. Chalmers, Sheffield Academic Press, Sheffield, 2000.
49 R. A. Nyquist, *Interpreting Infrared, Raman, and Nuclear Magnetic Resonance Spectra*, Academic Press, San Diego, CA, USA, 2001.
50 A. De Santis and M. Baldi, *Polymer*, 2004, **45**, 3797.
51 D. Lin-Vien, N. B. Colthup, W. G. Fateley and J. G. Grasselli, *Handbook of Infrared and Raman Characteristic Frequencies of Organic Molecules*, Academic Press, San Diego, CA, USA, 1991, 477.
52 C. A. McGill, A. Norden and D. Littlejohn, *Analyst*, 2002, **127**, 287.
53 M. A. Gauthier, I. Stangel, T. H. Ellis and X. X Zhu, *Biomaterials*, 2005, **26**, 6440.
54 L. Rey, J. Galy, H. Sautereau, G. Lachenal, D. Henry and J. Vial, *Appl. Spectrosc.*, 2000, **54**, 1, 39.
55 A. G. Mikos, C. G. Takoudis and N. A. Peppas, *Macromolecules*, 1986, **19**, 2174.
56 J. P. Fouassier, *Photoinitiation, Photopolymerization, and Photocuring: Fundamentals and Applications*, Carl Hanser Verlag, Munich, 1995.